Process-Monitoring Using Part Shape-Scales with Neural Networks: A Circular-Component Case

Kuang-Han Hsieh [a] and C. Alec Chang [b*]

[a] *Department of Management Science, Chinese Military Academy,
Fengshan, Kaohsiung 830, Taiwan, R.O.C.*
[b] *Department of Industrial and Manufacturing Systems Engineering,
University of Missouri-Columbia,
E3437 Engineering Building East, Columbia, MO 65211, U. S. A.*

Abstract: Existing approaches for conducting a control task for components machining generally include three methods: dimensional measurement, tolerance verification and equipment monitoring. However, spatial parameters from direct measurement present limited information about geometric features. Thus, many process monitoring systems must rely on acoustic information, torque and force sensors, vibration sensors, or an analysis of collected chips from a production process. These sensors can only detect problems caused by abnormal contact conditions between process tools and workpieces but not geometric deformations of industrial components produced in normal machining.

Frequency parameters that directly utilize coordinate data from an object can identify more detailed geometric features for the purpose of industrial process monitoring. Accordingly, many more process anomalies about manufacturing facilities can be revealed using neural networks to map geometric anomalies. This paper develops shape-scales extracted from Fourier descriptors from incoming part scans. By using these shape-scales, a pattern vector can be formed and fed into a feedforward neural network to identify error patterns. Also, using control charts, the identification of a process resetting point with shape-scales can be monitored. Since roundness is a recurring geometric form of industrial components, the monitoring of circular shape is used as an implementation example to illustrate the proposed system. This proposed system offers an alternative to obtain more process information through processed products in addition to hardware sensors.

1. Introduction

For almost a century, quality control (QC) tools have mainly used measurements in spatial domains such as cut-length or diameter. These measured parameters are initially used for pass-fail screening according to engineering and control specifications. More recently, patterns of variation and cumulative data from these measured parameters are used with certain control charts to diagnose process deviations. Various control charts are developed for more sophisticated control functions for reset point identification [1-3]. However,

---

measurements from spatial domains present only part of the geometric information of an object. Although frequency domain data from varieties of sensors are sometimes used in signal processing, they have not been utilized much in geometric measurements directly related to manufacturing functions. During the past two decades, some researchers have shown that geometric parameters in frequency domains can be a very powerful additional tool in revealing detailed shape features [4-7]. These features include contour undulations, periodic or non-periodic waves and some other shape irregularities. The identification of these complex geometric features can supply much related information for process monitoring.

Specifically, computer vision systems and coordinate measuring machines (CMM) are familiar implements for inspection tasks. When coordinate data of edge points from an object is obtained by a computer vision system or CMM, a common approach is to use piecewise linear approximation to fit edge data points into polylines or compound curves to represent the object boundary. Then these geometric elements are measured for quality control purposes [8]. These measurement methods present geometric parameters in spatial domains. However, the numerous data-points of a part edge are two-dimensional frequency data on a coordinate system. Geometrical mathematics in frequency domains can utilize this data directly for representing detailed geometric shapes. Utilizing modern powerful and economical microcomputers with proper input-output mapping methods such as neural networks, this detailed geometric information can reveal many more process anomalies about manufacturing systems.

Furthermore, an automated on-line measurement monitoring system should not only identify the cause of an out-of-specification problem, but should also indicate a time and direction to reset process tools. Due to the limited information presented by spatial parameters from direct measurement, many process monitoring systems that detect operation defects must rely on acoustic information, torque and force sensors, vibration sensors, or an analysis of collected chips from a production process. For example, Rice and Wu [9] investigate the use of Homomorphic processors for acoustic emission information to estimate cutting process parameters. Rajmohan and Radhakrishnan [10] analyze collected chips in monitoring grinding processes. Lee [11] uses sensors to measure machine degradation and fault detection in the manufacturing process. Yang and Kwon utilize images of process tools to monitor flank wear and crater wear [12]. Others use these traditional sensors with modern algorithms to determine tool wear [13-19]. Sheikh [20] and Kuo and Cohen [21] establish tool reset and replacement strategies along with tool-wear monitoring. However, not all quality problems are caused by abnormal contact conditions between process tools and workpieces. For example, an oval formed from a distorted circle can be the results of setup errors rather than tool contact conditions in a two passes operation in the milling process [22]. Therefore, without a better analysis of workpiece features, many quality problems related to geometric routings and setup conditions cannot be properly identified.

The need for a measurement system that can distinguish error patterns and identify reset points in a production process from a variety of geometric anomalies in a machining part is very obvious. Since much of the knowledge of relationships between yielded error patterns and causes of process problems has been obtained from past experiences, an error pattern identification function can be very useful for tool and equipment maintenance and preservation of manufacturing processes. Therefore, there is a need to develop a procedure that can facilitate inferring the causes of process problems in production

and determining tool-reset points. This research report addresses the development of such a procedure.

2. Problem formulation for shape analysis

The cross-sectional contour of an incoming part edge that is scanned by a device can be expressed in an X-Y coordinate plane with a finite set of sequential points, $s_k \subset S$. These points can be indicated by pairs of X coordinates, x_k, and Y coordinates, y_k, as

$$S \equiv \{s_k = (x_k, y_k) \mid k \in \{1, 2, .., N\}\}, \qquad (1)$$

where N is the total number of points in S.

The problem solving task of this project becomes the development of a shape analysis procedure to conduct an error pattern identification function for parts by using S. In addition, this procedure, F, should also be able to conduct a reset point identification function as

$$F(S) \rightarrow (\text{error pattern}, \text{process reset point}). \quad (2)$$

This procedure can be further described as the following tasks:

From S shown in Eq. (1), a shape pattern vector, $\mathbf{V}$, can be obtained as

$$\mathbf{V} = C[E(S)] = [v_1, v_2, ...], \qquad (3)$$

where $\mathbf{V}$ is a shape pattern vector with c number of shape-scales v, E is a feature extraction function, and C is a collection of shape-scales.

We would like to use the shape pattern vector $\mathbf{V}$ to infer an error pattern i. This task could be expressed as

$$\mathbf{V} \Rightarrow \text{error pattern } i \quad \text{for } i \in \{1, 2, ..., q\}, \quad (4)$$

where q is the total number of potential error patterns in a manufacturing process.

In addition, we would also like to monitor the process by detecting a required process reset using $\mathbf{V}$ as

$$\mathbf{V}(t) \Rightarrow r, \qquad (5)$$

where $\mathbf{V}(t)$ is the shape pattern vector of an incoming part at the sequence t, and r is the inferred process reset point.

3. Proposed methods

In order to accomplish the above tasks, algorithms for a feature extraction procedure to conduct the task in Eq. (3), an identification procedure for the task shown as Eq. (4), and a reset point identification function to fulfill the task shown as Eq. (5) should be constructed. We propose that for the feature extraction procedure, the input is ordered boundary points of the incoming cross-sectional contour and the output can be the extracted shape pattern vector that consists of various shape-scales. For the error pattern identification procedure, the input is the formed pattern vector and the output should be the identified error pattern. By using the reset point identification function, the changing shape-scales through the sequence of incoming parts should indicate necessary process reset points.

3.1. Generating shape-scales from shape analysis

Since current methods using raw figures from direct measurement cannot provide sufficient shape features, a more precise analytical method is necessary to generate more detailed information for shape analysis. Many researchers suggest the Fourier Descriptor (FD) as an effective method for shape analysis. For example, Granlund [4] and Zahn and Roskies [5] use a normalized Fourier descriptors (NFD) algorithm to extract the effective feature for the purpose of pattern recognition.

Kuhl and Giardina [6] propose a Fourier-features-algorithm that is based on the information contained in the Freeman chain code. Lin and Hwang [7], and Lin and Jungthirapanich [23] also propose a modified form of invariant Fourier descriptors for pattern recognition. Leou and Tsai [24] and Yip *et al.* [25] apply Fourier descriptors to detect shape symmetry. Chang *et al.* [26] use FDs with excellent results to infer the position information for bar codes on products to be handled. Therefore, to accomplish the task shown in Eq. (3), FD base methods are adopted as the feature extraction function to obtain shape pattern vector **V**. The process of using FDs to compute various shape-scales, $v_k \subset \mathbf{V}$, is summarized as follows:

The coordinate set of the cross-sectional contour of incoming parts, $S=\{(x_1,y_1),...,(x_N,y_N)\}$, is generally obtained from computer vision systems, coordinate measurement machines or other devices. The Fourier descriptors, $a(n)$, can be extracted by applying discrete Fourier transform to S as

$$a(n) \cong \frac{1}{N} \sum_{m=0}^{N-1} u(m) e^{(-j2\pi nm/N)} , n \in \{0,1,...,N\text{-}1\}, \quad (6)$$

where $u(m) = x_m + jy_m$, $m=1,2,..,N$, $j = \sqrt{-1}$, and the inverse Fourier transform of $a(n)$ which restores $u(m)$, is

$$u(m) \cong \sum_{n=0}^{N-1} a(n) e^{(j2\pi nm/N)} , m \in \{0,1,...,N\text{-}1\}. \quad (7)$$

To conduct shape analysis tasks, algorithms from Mitchell and Kim [27] and Grogan and Mitchell [28] can be further developed according to the geometry of parts to obtain shape-scales from extracted FDs.

By using proper shape-scales, the shape information for an incoming part feature can be obtained. Then a shape pattern vector, **V**, can be constructed by various shape-scales as

$$\mathbf{V} = [v_1, v_2, ...] \quad (8)$$

This shape pattern vector can be used as input information to facilitate the error pattern identification process and reset point identification task.

3.2. Error pattern identification from shape pattern vector

An identification function using the information from various shape-scales is needed to identify error patterns as shown in Eq. (4). Among existing algorithms for this type of task, statistical methods, knowledge-based systems and artificial neural networks can be considered, such as by Kourti *et al.* [29], Kourti and MacGregor [30], Lee [31], and Lennox [32]. Specifically, neural networks do not require articulation of the underlying probability distribution functions in order to map a dependency function from inputs. Among various artificial neural networks, the feedforward neural network is the most frequently adopted algorithm based on its excellent ability to learn mapping of input and output patterns. For example, Chang and Su [33] elaborate the use of feedforward neural networks to model error patterns in measurement without the need for prior error distributions. Therefore, a feedforward neural network is adopted to conduct the error pattern identification function in this project.

Using experimental data or previous records from a manufacturing process, a feedforward neural network can be structured to map different contour data and their corresponding errors. Then, this neural network can be utilized to identify error patterns in a process. This identification task can be described as

$$N[\mathbf{V}] \rightarrow \mathbf{P} = [p_1, p_2, .., p_q], \quad (9)$$

where N is a structured feedforward neural network from experimental data, **P** is the measurement vector of error patterns, p, which is associated with output nodes of the constructed neural system, and q is the desig-

nated number of error patterns to be identified in a manufacturing process.

Thus error patterns of a circular part can be identified as

$$\{\text{For } \forall p_l \in \mathbf{P}, \exists p_i > \mathsf{Z}\} \rightarrow \text{error pattern } i, \quad (10)$$

where Z is a predetermined threshold value for an error pattern.

When an error pattern is identified, process causes of this error can be explored.

3.3. Reset point identification

To monitor whether the process setting is deteriorating through time, a reset point iden-tification function utilizing the data of shape changes from incoming parts is proposed. An effective method to observe these changes in sampling datum is using control charts. Dif-ferent control charts can be utilized to super-vise respective shape-scales that represent various shape information in a real-time reset point identification function. Designated shape-scales for this control function are based on their sensitivity for each industrial process. A control chart for each chosen shape-scale can be constructed by an upper process control limit (UCL) and a lower proc-ess control limit (LCL) to indicate process resetting regions. The UCL and LCL for des-ignated shape-scales should be specified by process engineers.

If a shape-scale has entered a predeter-mined resetting region in an industrial process, the action of process resetting or other main-tenance procedures should be triggered (Fig-ure 1). This procedure can be expressed as:

Let the resetting region

$$Q(v_k) = \{v_k | v_k \in \mathbf{V}, v_k \le v_k^L \cup v_k \ge v_k^U\}, \quad (11)$$

then $v_k(t) \in Q(v_k) \rightarrow r$,

where $v_k(t)$ is kth shape-scale of tth incoming part, v_k^L is the lower control limit (LCL) of v_k, v_k^U is the upper control limit (UCL) of v_k, and r is the identified process reset point of the incoming part sequence.

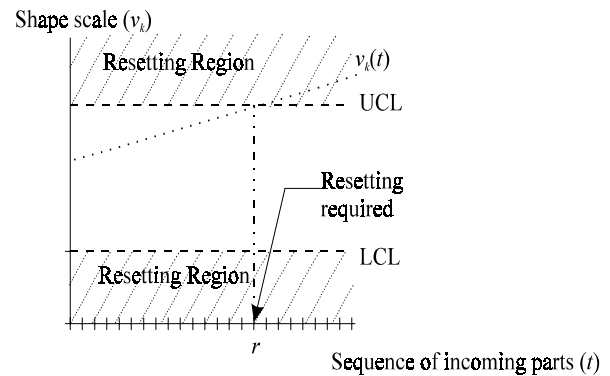This proposed procedure in Eq. (11) can fulfill the task specified in Eq. (5).

Figure 1. An example of using the proposed proc-ess monitoring method

3.4. Summary of the proposed method

These proposed methods can fulfill the tasks of error pattern identification and reset point identification in a manufacturing envi-ronment. An integrated monitoring procedure based on these methods can be summarized in Figure 2.

4. Implementation for circular-components

Since roundness is a frequently recurring geometric form of manufactured components, it is used as an implementation example to illustrate this proposed procedure. The con-ventional method for inspecting the roundness of the cross-sectional contour of a part is to measure the difference between the largest
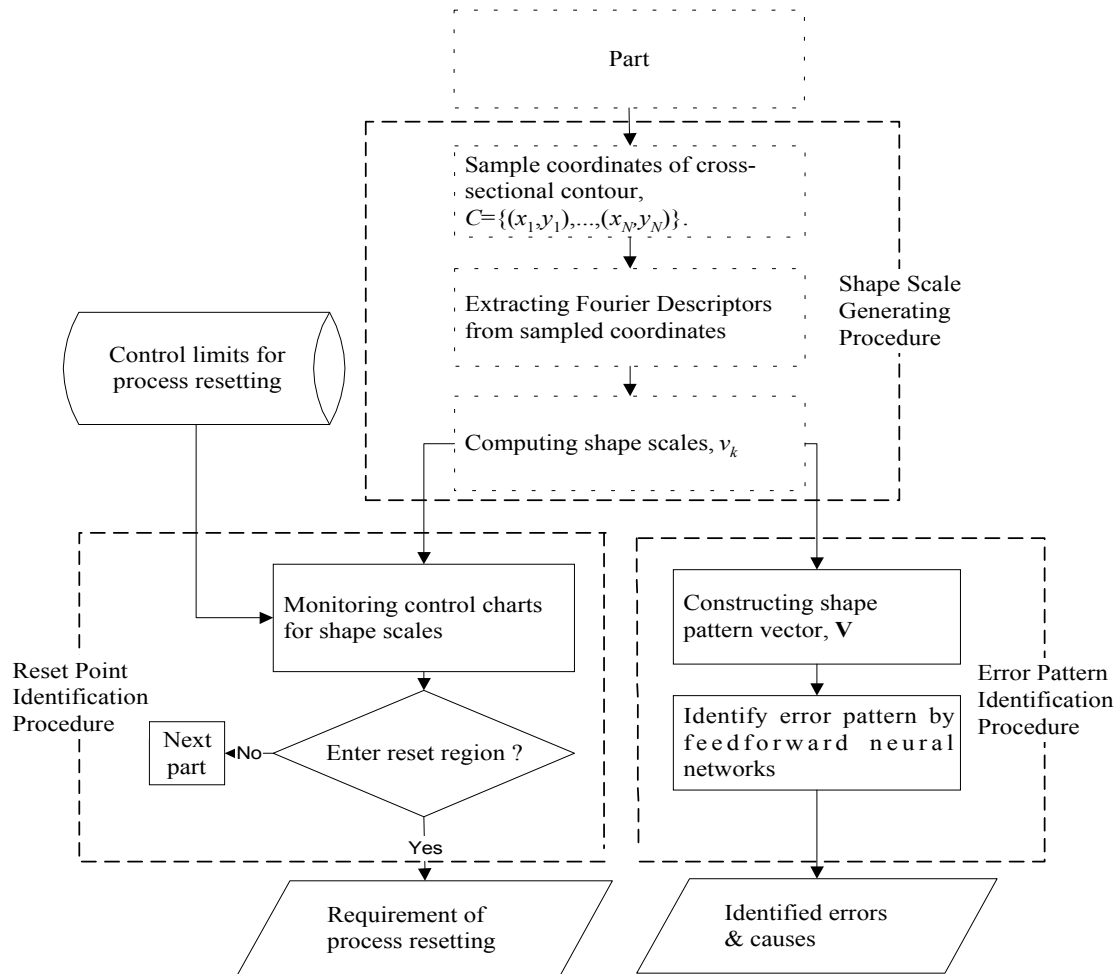
Figure 2. The framework of proposed procedures

and the smallest radii and compare these measurements with design specification. These radii are obtained by defining a center using minimum radial separation criterion, least-squares curve fitting, maximum inscribed circle, or minimum circumscribed circle etc. [34]. These roundness inspection methods are usually categorized into two tasks based on their goals: dimensional measurement and verification of tolerance specification. From the task of dimensional measurement [35-36], the elementary measurement information provided by existing algorithms is not sufficient in distinguishing many potential process problems. For the task of verification of tolerance specification, computational geometry algorithms, optimization approaches and statistical inference are the most frequently adopted methods [37-41]. However, these methods are not developed to carry out process monitoring tasks for their corresponding industrial processes. A more precise analysis of circular shape according to the proposed method is required.

4.1. Shape-scales for circular components

To conduct better shape analysis tasks that facilitate the process monitoring job, algorithms from Mitchell and Kim [27] and Grogan and Mitchell [28] are further developed to calculate different shape-scales from extracted FDs. Various shape-scales are de-

rived for process monitoring of circular components.

4.1.1. Circularity and radius scales

There are only two FD terms, $a(0)$ and $a(1)$, that are non-zero for a perfect circle. $a(0)$ represents the location of the center and $|a(1)|$ represents the radius. Otherwise, there would be additional non-zero terms for a non-perfect circle. The sum of their absolute values, $\sum_{n,n\neq0,1}|a(n)|$, increases as the circular shape deteriorates. Therefore, information from these non-zero terms describes how this circle deviates from a perfect circle. The circularity scale of a common circular feature can be defined by the ratio of the $|a(1)|$ and $\sum_{n,n\neq0}|a(n)|$ as

$$Circularity\ Scale = \frac{|a(1)|}{\sum_{n,n\neq0}|a(n)|}, \qquad (12)$$

and the radius scale can be defined as

$$Radius\ Scale = |a(1)|. \qquad (13)$$

4.1.2. Axial symmetry scale

Axial symmetry means the shape is symmetric in any direction about its center. In general, for a perfect axially symmetrical feature, odd FD terms are non-zero and even FD terms are zero. For a non-perfect axially symmetrical feature, the even terms become non-zero and the sum of their absolute values increases as the axial symmetry deteriorates. Therefore, for a common circular feature, the axial symmetry scale can be defined by the ratio of the absolute sum of odd FDs and the absolute sum of total FDs, $\sum_{n,n\neq0}|a(n)|$, as

$$Axial\ Symmetry\ Scale = \frac{\sum_{n=odd\ number}|a(n)|}{\sum_{n,n\neq0}|a(n)|} . \qquad (14)$$

4.1.3. Bilateral symmetry scale

When a shape is symmetric about a line, it exhibits bilateral symmetry. If a perfect bilaterally symmetrical shape is rotated about the line of symmetry by using phase normalization of FDs, its FD terms are all real. For a non-perfect bilaterally symmetrical feature, the imaginary parts of FDs become non-zero and the sum of their absolute values increases as the bilateral symmetry deteriorates. Thus, the bilateral symmetry scale can be defined as

$$\begin{aligned} &Bilateral Symmetry Scale \\ &= \frac{\sum_{n,n\neq0}|R[a(n)]|}{\sum_{n,n\neq0}\{|R[a(n)]|+|I[a(n)]|\}}, \end{aligned} \qquad (15)$$

where $R[a(n)]$ is the real part of the complex number $a(n)$, and $I[a(n)]$ is the imaginary part of the complex number $a(n)$.

A simple way of phase normalization is to make the phase of $a(1)$ and $a(N-1)$ equal to zero by applying its rotation angle and shafting distance. Since the FDs repeat periodically, $a(-1)$ is used to replaced $a(N-1)$ in the following two equations. The rotation angle, θ, and shafted distance of the starting point, η, can be obtained from the following equations as

$$\theta = \frac{-1}{2}\left\{\tan^{-1}\left(\frac{I[a(1)]}{R[a(1)]}\right)+\tan^{-1}\left(\frac{I[a(-1)]}{R[a(-1)]}\right)\right\}, \qquad (16)$$

$$\eta = \frac{N}{4\pi}\left\{\tan^{-1}\left(\frac{I[a(1)]}{R[a(1)]}\right)-\tan^{-1}\left(\frac{I[a(-1)]}{R[a(-1)]}\right)\right\}. \qquad (17)$$

4.1.4. Ellipticity scale

Since elliptical distortion is a common defect in various circularity production processes, it should be measured in a shape analysis task of circular part features. For a perfect elliptical feature, there are only two non-zero FDs, $a(1)$ and $a(N-1)$. In addition, letting A and B be semi-axis lengths of a perfect elliptical feature, we have $a(1) = (A+B)/2$ and $a(N-1)= (A-B)/2$. If A equals B, the ellipse feature becomes a circle rather than an ellipse. Therefore, an elliptical scale that represents how an elliptical feature departs from a perfect circle can be defined as

$$Ellipticity\ Scale = \frac{A}{B} = \frac{a(1) + a(N-1)}{a(1) - a(N-1)}. \qquad (18)$$

4.1.5. *K*-fold rotational symmetry scale

If a centerless grinding is inadequately controlled, this process tends to generate circular forms with angularity that is characterized by an odd number of similarly spaced undulations. The K-fold rotational symmetry is a corresponding descriptor for these distortions due to generated undulations. Therefore, the K-fold rotational symmetry should be included in a shape analysis task of circular part features. For an exact K-fold rotationally symmetrical object, $a(n)$ has the following property:

$a(n) \neq 0$, only if $(n-1)\,\mathrm{mod}\,K = 0$, and

$a(n) = 0$, for all other n.

If the K-fold rotational symmetry of a circular feature deteriorates, the sum of the absolute values of $a(n)$ terms, where $n \neq 0$ and $(n-1)$ mod $K=0$, increases. Thus, the K-fold rotational symmetry can be defined as

K-fold Rotational Symmetry Scale

$$= \frac{\sum\limits_{n=l,(l-1)\bmod K=0,l\neq 0,l\neq 1}|a(n)|}{\sum\limits_{n,n\neq 0}|a(n)|}. \qquad (19)$$

4.1.6. Zigzag scale

The zigzag distortion is a frequently occurring defect in various production processes due to inadequate positioning of workpieces or tools. Based on the property of Fourier transform, major shape information of circular features, such as location of the center and the radius, is associated with the low frequency area of FDs. Noise such as the zigzag phenomena generates FDs in a high frequency area. By observing the ratio of the sum of the absolute high frequency FD terms and the sum of the total absolute FDs, the zigzag distortion can be estimated. Therefore, the zigzag scale can be defined by the relative magnitude of the high frequency area in the center section of FDs:

$$Zigzag\ Scale = \frac{\sum\limits_{n=M/2}^{N-1-M/2}|a(n)|}{\sum\limits_{n,n\neq 0}|a(n)|}, \qquad (20)$$

where FDs before the ($M/2$)th term and after the (N-1-$M/2$)[th] term in the numerator are discarded, and M is determined experimentally.

4.2. Constructing shape pattern vector

The experimental part feature is a circular hole with a two inch radius. Corresponding testing templates that have gradually increasing deformations are generated for every type of error pattern. These testing templates are then scanned by a computer vision system to obtain contour coordinates. Other equipment includes: 1) PULNIX TM-54 CCD; 2) SONY CPD-1310 NTSC monitor; 3) DATA TRANSLATION DT2803 frame grabber board; and 4) Pentium based PC. In order to demonstrate the proposed procedure, part templates with deformed characters (error patterns) due to the drilling process such as oversize, ellipticity, oval, and zigzag are used. For zigzag error patterns, random irregularities and consistent undulations are included.

The coordinates of the contour, $S=\{(x_1,y_1), (x_2,y_2),..., (x_N,y_N)\}$, are sampled in a counter-clockwise direction as
$S=\{ (101,205),(102,204),...,(221,203),(221,204),(222,205),...,(101,207),(101,206) \}$.

The various shape-scales, $v_k \subset \mathbf{V}$, of this incoming part feature are obtained by applying Eq. (6) and Eq. (12) through Eq. (20). As the following example demonstrates, these shape-scales are then used to form a shape pattern vector:

$$\mathbf{V} = [v_1, v_2, v_3, v_4, v_5, v_6]$$
$$= [\textit{Circularity, Ellipticity, Axial sym.,}$$
$$\textit{Bilateral sym., Zigzag, Radius }]$$
$$= [0.8485, 1.0045, 0.9357, 0.9337, 0.1016,$$
$$106.3497].$$

4.3. Error pattern identification procedure

A feedforward neural network is trained by a set of collected data that includes many patterns of potential deformation types occurring in drilling processes. During the training stage, the target value of each $p \in \mathbf{P}$ is set to be 1 to represent an associated error pattern or 0 to represent the nil of that associated error pattern. When sets of input patterns and output target patterns are given to different structures of the neural networks as training sets, the weights of structural nodes keep adjusting to reduce the difference between the outputs of network and target patterns. During this training stage, forward pass and backward pass are conducted layer by layer for each pair of input pattern ($\mathbf{V}$) and output target vector ($\mathbf{P}$). At the end of each forward pass, an error function is formed based on the difference between the target value and actual output value. A gradient incremental function is then applied to adjust the weights in the backward pass. Then a forward pass is conducted again using the adjusted weights. These steps are repeated until the differences between the outputs and target patterns of one type of network structure efficiently converge to pre-determined levels.

This network with the trained weights of all nodes can be used to estimate the output of new incoming input patterns by only passing information forward through the nodes. As shown in Eq. (9), the shape pattern vector, $\mathbf{V}$, is used as input for this trained feedforward neural network for the error pattern identification function. The occurred error pattern is identified from the output $\mathbf{P}$ as shown in Eq. (10):

$$N[\mathbf{V}] \rightarrow \mathbf{P} = [p_1, p_2, p_3, p_4, p_5]$$
$$=[\textit{Measurement of Circularity,}$$
$$\textit{Measurement of Oversize,}$$
$$\textit{Measurement of Ellipticity,}$$
$$\textit{Measurement of Oval,}$$
$$\textit{Measurement of Zigzag}]$$
$$=[-0.010, 0.001, 0.008, 0.020, 1.027]$$

Since the threshold, Z is predefined as 0.50, we can conclude
$$\{ \exists p_5 > Z \} \quad \rightarrow \quad \text{error pattern}: \textit{Zigzag}.$$
That is, the identified error pattern is $\textit{Zigzag}$ since its $\textit{Zigzag}$ scale, $p_5= 1.027 > Z$.

The structure of the neural networks is provided in Figure 3. A 6-8-5 structure produces excellent results for this implementation example.

4.4. Reset point identification procedure

By utilizing control charts, the changes of shape-scales corresponding to deformations can be monitored. Whenever any shape-scale enters the process resetting zone in a control chart, a process resetting or related maintenance jobs should be triggered. Based on the sensitivity of various shape-scales for the drilling process in this implementation example, the ellipticity, bilateral symmetry, zigzag and radius scales are chosen to be monitored. The ellipticity scale is used to monitor elliptical deformations that can result from misalignment of the drill chuck and surface da-

tum. Bilateral symmetry scale is selected to

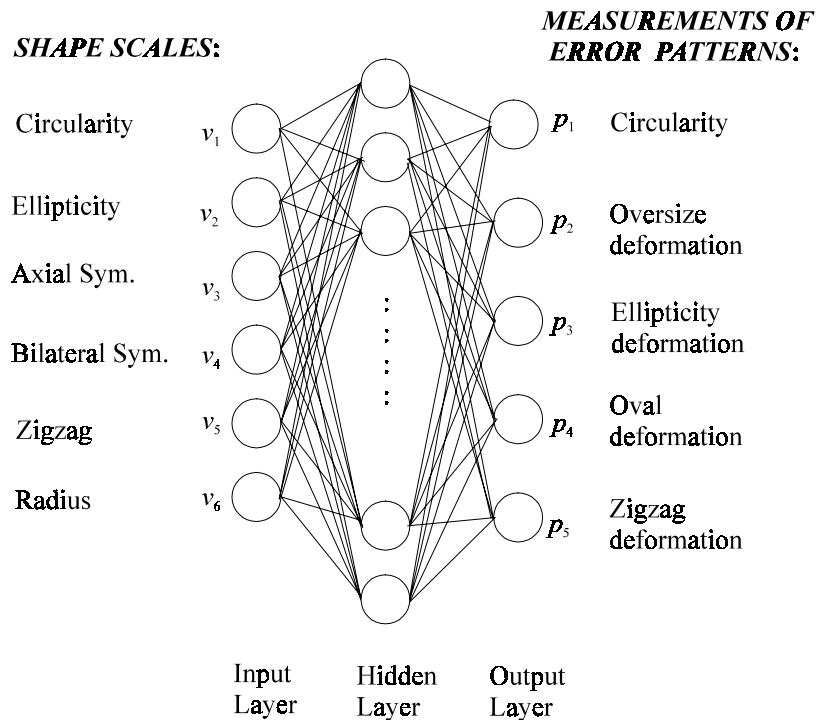supervise oval deformations that are produced

Figure 3. Feedforward neural network for error pattern identification of circular components

by inaccurate drill centers or worn-out center holes. The zigzag scale is adopted to audit diverse zigzag deformations that are induced by inadequate stability in the work positioning and holding, etc. The radius scale is used to track the size problems that can be caused by tool wear or misalignment of rotational angle. Other shape deformations are less frequent in drilling processes.

Using the procedure as shown in Eq. (11), we have obtained the following result in simulated data:

$$\{\exists v_5(\#21) \geq v_5^U\}$$
$$\rightarrow r = \text{sequence } \#21 \text{ of incoming part}$$

where $v_5(\#21)$ is the *Zigzag* scale of incoming part #21, $v_5^U = 6.5450$, the upper control limit (UCL) of the *Zigzag* scale, and r is the reset point of the incoming part sequence.

As shown in Figure 4, this imbedded reset point is correctly identified by the proposed procedure.

5. Conclusions

By using the error pattern identification function of the proposed method that includes all related shape-scales, many circular deformations other than radius variation can be detected. By utilizing the proposed method, not only can deformations other than radius variation be recognized but the process resetting point is also provided. This situation is illustrated in the implementation example as shown in Figure 4. It is obvious that by measuring only the radii, other process problems cannot be detected as shown in Figure 4(d). The radii of continuously incoming parts are within the control limits, but the zigzag scale of the same incoming part #21 is out of control as shown in Figure 4(c). Since we can trace potential causes from the change in shape-scales, we will be able to reset process equipment accordingly (Table 1, adopted
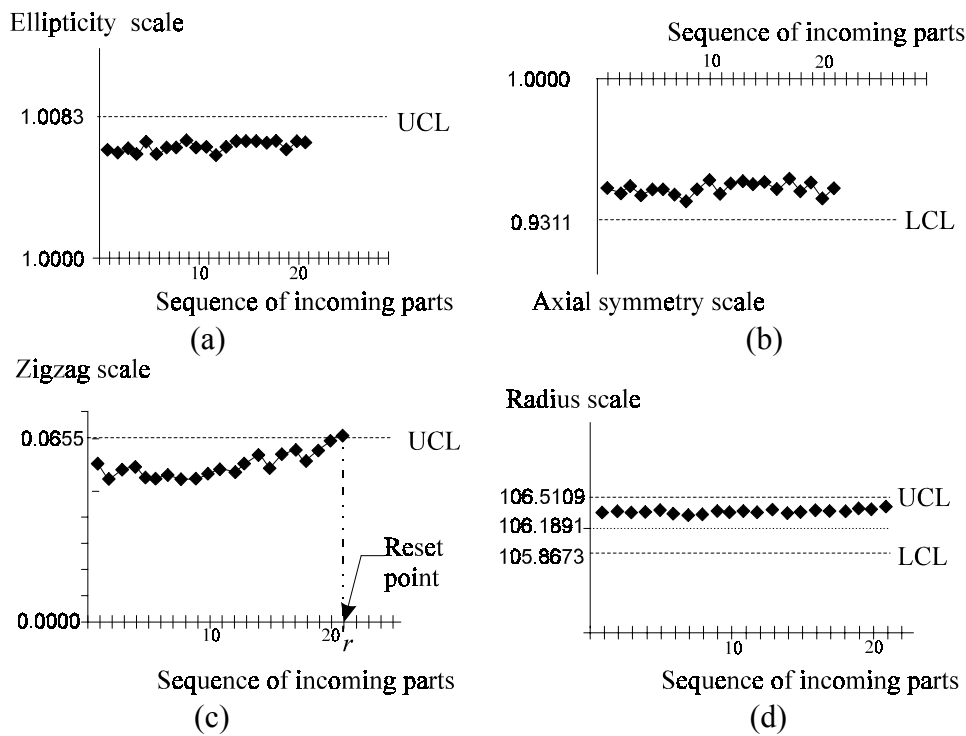
from Farago [34], Drozda and Wick [42]).
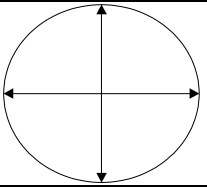
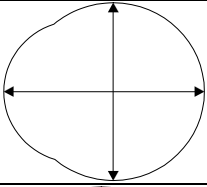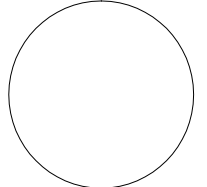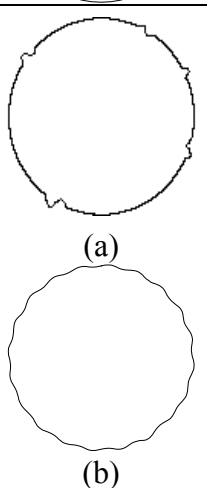Figure 4. Control charts for process resetting

Thus, the action of process resetting or maintenance can be triggered to correct the following problems: (1) inadequate stability in the work positioning and holding, or (2) improper setup and insufficient rigidity of the workpiece.

The proposed error pattern identification procedure and reset point identification function ally Fourier descriptor methods and artificial neural networks effectively. They overcome the drawbacks of many existing process monitoring methods that can only detect the problems caused by abnormal contact conditions between process tools and workpieces. This proposed procedure is implemented in experimental settings for circular components that are representative of practical situations in industrial processes. It provides an assurance for the quality of the yielded product and equipment performance. In addition, this proposed method can be applied to diverse industrial operations by using different sets of shape-scales. For example, we can add the proposed K-fold rotational symmetry shape-scale to those in our drilling process case for the centerless grinding process.

In conclusion, control parameters from spatial domains present limited geometric information that is not sufficient for modern industrial technology. In traditional inspection tasks, engineers designate the measurement of parts using length, radius, etc. These measurements do not supply sufficient information regarding error patterns in part features. For example, in a drilling process, the existing dimensional measurement methods can only provide the radii of circular features. They cannot reveal other causes of circular deformations. In order to obtain more shape information for monitoring purposes, the proposed parameters from frequency domains must be utilized. When coordinate data of

Table 1. Error patterns of drilling process and their potential causes

Exaggerated Diagram	Error Pattern	Description	Potential Causes
	Ellipse	Unequal length of two perpendicular axes that are symmetrically located.	Misalignment of drill chuck and surface datum.
	Oval	Egg shaped, essentially oval yet the major and minor axes are not symmetrically located.	Inaccurate drill centers and/or worn-out center holes.
	Change of size	Change of radius.	Tool wear or misalignment of rotational angle.
(a) (b)	Zigzag	(a) Random irregularities characterized by non-periodic departures from the basic round form. (b) Contour undulations (medium frequency lobing). Departures from the basic round form that are essentially consistent in spacing and amplitude.	(a) Frequently associated with inadequate stability in the work positioning and holding. (b) Vibrations of drill bit due to improper setup, and insufficient rigidity of the workpiece.

edge points from an object is obtained, geometrical mathematics using frequency domains can directly utilize this data to represent geometric features of part edges. Thus, industrial practitioners can obtain more detailed geometric features. Utilizing modern computers with excellent input-output mapping methods such as neural networks, this detailed geometric information can reveal many more process anomalies about manufacturing systems.

The use of frequency parameters and neural networks for industrial processes is relatively new to production engineers due to its need for economical computer power that is not available before. However, its theoretical background has been well established for two decades. In addition to hardware sensors, this proposed system offers additional methods to generate process information through processed products.

References

[1] Reynolds, M. R. Jr. and Stoumbos, Z. G. 1998. SPRT chart for monitoring a proportion. *IIE Transactions*, 30: 545-561.

[2] Gultekin, M., Elsayed, E. A., English, J. R., and Hauksdottir, A. S. 2002. Monitoring automatically controlled processes using staticstical control charts. *International Journal of Production Research*, 40: 2303-2320.

[3] Elasayed, E. A. and Chen, A. 2000. An alternative mean estimator for processes monitored by SPC charts. *International Journal of Production Research*, 38: 3093-3109.

[4] Granlund, G. H. 1972. Fourier processing for hand printed character recognition. *IEEE Transactions on Computers*, 21: 195-201.

[5] Zahn, C. T. and Roskies, R. Z. 1972. Fourier descriptors for plane closed crves. *IEEE Transactions on Computers*, 21: 269-281.

[6] Kuhl, F. P. and Giardina, C. R. 1982. Elliptic Fourier features of a closed contour. *Computer Graphics and Image Processing*, 18: 236-258.

[7] Lin, C. S. and Hwang, C. L. 1987. New forms of shape invariants from elliptic Fourier descriptors. *Pattern Recognition*, 20: 535-545.

[8] Tien, F. C. and Chang, C. A. 1999. Using neural networks for 3d measurement in stereo vision inspection systems. *International Journal of Production Research*, 37: 1935-1948.

[9] Rice, J. A. and Wu, S. M. 1994. Acoustic emission source and transmission path characterization through homomorphic processing. *Journal of Engineering for Industry*, 116: 32-41.

[10] Rajmohan, B. and Radhakrishnan, V. 1994. On the possibility of process monitoring in grinding by spark intensity measurements. *Journal of Engineering for Industry*, 116: 124-129.

[11] Lee, J. 1995. Modern computer-aided maintenance of manufacturing equipment and systems: review and perspective. *Computers & Industrial Engineering*, 28: 793-811.

[12] Yang, M. Y. and Kwon, O. D. 1998. A tool condition recognition system using image processing. *Control Engineering Practice*, 6: 1389-1395.

[13] Kumar, S. A., Ravindra, H. V., and Srinivasa, Y. G. 1997. In process toll wear monitoring through time series modeling and pattern recognition. *International Journal of Production Research*, 35: 739-751.

[14] Choudhury, S. K., Jain, V. K., and Rao, R. 1999. On-line monitoring of tool wear in turning using a neural network. *International Journal of Machine Tools & Manufacture*, 39: 489-504.

[15] Ghasempoor, A., Moore, T. N., and Jeswiet, J. 1998. On-line wear estimation using neural networks. *Journal of Engineering Manufacture*, 212: 105-112.

[16] Sick, B. 2002. Fusion of hard and soft computing techniques in indirect, online tool wear monitoring. *IEEE Transactions on Systems, Man and Cybernetics Part C: Applications and Reviews*, 32: 80-91.

[17] Purushothaman, S. and Srinivasa, Y. G. 1998. A procedure for training and artificial neural network with application to tool wear monitoring. *International Journal of Production Research*, 36: 635-651.

[18] Li, X. 2002. A brief review: acoustic emission method for tool wear monitoring during turning. *International Journal of Machine Tools and Manufacture*, 42: 157-165.

[19] Everson, C. E. and Hoessein, C. S. 1999. The application of acoustic emission for precision drilling process monitoring.

International Journal of Machine Tools & Manufacture, 39: 371-387.

[20] Sheikh, A. K. 1999. Optimal tool replacement and resetting strategies in automated manufacturing systems. *International Journal of Production Research*, 37: 917-937.

[21] Kuo, R. J. and Cohen, P. H. 1999. Multi-sensor integration for on-line tool wear estimation through radial basis function networks and fuzzy neural network. *Neural Networks*, 12: 355-370.

[22] Sarma, S. E. and Wright, P. K. 1996. Algorithms for the minimization of setups and tool changes in "simply fixturable" components in milling. *Journal of Manufacturing Systems*, 15: 95-112.

[23] Lin, C. S. and Jungthirapanich, C. 1990. Invariants of three-dimensional contours. *Pattern Recognition*, 23: 833-842.

[24] Leou, J. J. and Tsai, W. H. 1987. Automatic rotational symmetry determination for shape analysis. *Pattern Recognition*, 20: 571-582.

[25] Yip, R. K. K., Tam, P. K. S., and Leung, D. N. K. 1994. Application of elliptic fourier descriptors to symmetry detection under parallel projection. *IEEE Transactions on Pattern Analysis and Machine Intelligence*, 16: 277-286.

[26] Chang, C. A., Lo, C. C., and Hsieh, K. H. 1997. Neural networks and fourier descriptors for part positioning using bar code features in material handling systems. *Computers Ind. Engng*, 32: 467-476.

[27] Mitchell, O. R., Kim, H. S., Grogan, T. A., and Kuhl, F. P. 1991. Fourier descriptor based generic shape recognition. *Technical Paper ACSM-ASPRS Annual Convention (Baltimore, MD.)*, 5: 279-278.

[28] Grogan, T. A. and Mitchell, O. R. 1983. Shape recognition and description: a comparative study. "*Technical Report TR-EE 83-22*", School of Electrical Engineering, Purdue University.

[29] Kourti, T., Nomikos P., and MacGregor, J. F. 1995. Analysis, monitoring and fault diagnosis of batch processes using multi-block and multiway PLS. *Journal of Process Control*, 5: 277-284.

[30] Kourti, T. and MacGregor, J. F. 1996. Multivariate SPC methods for process and product monitoring. *Journal of Quality Technology*, 28: 409-428.

[31] Lee, J. 1996. Measurement of machine performance degradation using a neural network model. *Computers in Industry*, 30: 193-209.

[32] Lennox, B., Montague, G. A., Frith, A. M., Gent, C., and Bevan, V. 2001. Industrial application of neural networks-an investigation. *Journal of Process Control*, 11: 497-507.

[33] Chang, C. A. and Su, C. T. 1995. A comparison of statistical regression and neural network methods in modeling measurement errors for computer vision inspection systems. *Computers & Industrial Engineering*, 28: 593-603.

[34] Farago, F. T., 1982. "*Handbook of dimensional measurements*". 2nd Ed., Industrial Press, New York.

[35] Yeralan, S. and Ventura, J. A. 1988. Computerized roundness inspection. *International Journal of Production Research*, 26: 1921-1935.

[36] Chen, J. M. and Ventura, J. A. 1995. Vision-based shaped recognition and analysis of machined parts. *International Journal of Production Research*, 33: 101-135.

[37] Etesami, F. and Qiao, H. 1990. Analysis of two-dimensional measurement data for automated inspection. *Journal of Manufacturing systems*, 9: 21-34.

[38] Roy, U. and Zhang, X. 1994. Development and application of voronoi diagrams in the assessment of roundness error in an industrial environment. *Com-*

puters & Industrial Engineering, 26: 11-26.

[39] Roy, U. 1995. Computational methodologies for evaluating form and positional tolerances in a computer integrated manufacturing system. *International Journal of Advanced Manufacturing Technology*, 10: 110-117.

[40] Car, K. and Ferreira, P. 1995. Verification of form tolerances part II: cylindricity and straightness of a median line. *Precision Engineering*, 17: 144-156.

[41] Kurfess, T. R. and Banks, D. L. 1995. Statistical verification of conformance to geometric tolerance. *Computer Aided Design*, 27: 353-361.

[42] Drozda, T. J. and Wick, C., 1983. "*Tool and manufacturing engineers handbook*". 4th Ed., Society of Manufacturing Engineers, Dearborn MI.